Simulation-based seasonal underground sensible heat storage integrated in a district heating network

ter Meulen, Bram; Geerts, Rene ; Infante Ferreira, C.A.

DOI
10.34641/clima.2022.309

Publication date
2022

Document Version
Final published version

Published in
CLIMA 2022 - 14th REHVA HVAC World Congress

Simulation-based seasonal underground sensible heat storage integrated in a district heating network

Bram ter Meulen [a], *Rene* Geerts [b], *Carlos* Infante Ferreira [c].

[a] Department Process & Energy, Faculty of Mechanical, Maritime & Materials Engineering, Delft University of Technology, Delft, the Netherlands, bramtermeulen@gmail.com.

[b] Hocosto BV, Zundert, the Netherlands, r.geerts@hocosto.com.

[c] Department Process & Energy, Faculty of Mechanical, Maritime & Materials Engineering, Delft University of Technology, Delft, the Netherlands, c.a.infanteferreira@tudelft.nl.

Abstract. This study assesses the role of (seasonal) thermal energy storage in the next generation renewables based central heating systems for the built environment in the Netherlands. Specifically, the neighbourhood "Karwijhof" in the city Nagele which is transitioning to a collective renewable district heating network incorporating 24 users. The study focus on the technology for storing thermal energy and two different heat collection technologies. The storage of heat is done using an underground seasonal thermal energy storage (USTES), in this case an underground sensible heat storage tank using water as storage medium. The system relies on a small scale district heating network (DHN) for the distribution of heat. For this research two heat collection technologies are considered both incorporating the USTES as main system component. The first system relies on heat collection by solar thermal collectors, the second on an air-water heat pump. Both systems are modelled in Matlab-Simulink making use of KNMI weather data. Different system sizes are evaluated. The investigated components include: volume of the USTES, surface area of the solar thermal collectors, and air-water heat pump capacity. Key performance indicators include the levelised cost of heat (LCOH) and the seasonal COP of the system which gives an indication on the autonomy of the system. To increase the autonomy of the systems a photo-voltaic (PV) array is considered for both systems to offset the electricity use. However, the systems are allowed to exchange electricity with the grid translating into the goal of "zero on the meter" autonomy. The results show that both systems can ensure heat throughout the year for the users considered during this study. However, systems cannot compete with traditional natural gas heating systems based on the LCOH. This is partly due to the high cost of the district heating network. The systems including a PV array show a LCOH that can compete with the traditional natural gas HR-boiler but are constraint by the rooftop area available during this study leading to a non-competitive LCOH. When considering the environmental benefits, the systems are already competitive to the traditional natural gas heating systems.

Keywords. Energy, Renewable and smart energy solutions for buildings and sites, Design of Innovative HVAC systems for optimized operational performances.
DOI: https://doi.org/10.34641/clima.2022.309

1. Introduction

In recent years climate change has gained more awareness among the public and has become an everyday important topic in regional and world politics. Due to the Paris and Glasgow climate agreements of, respectively, 2016 and 2021 the pressure to transition to a sustainable and renewable energy future has been increasing.

Since the Paris agreement countries have been moving towards even more ambitious goals on reducing their greenhouse gas emissions and increase energy efficiencies. In Europe this resulted in the proposition of the 'European Green Deal' setting ambitious goals for various energy consuming sectors including the energy efficiency of the built environment. On this topic the European Commission stated: "The Commission will rigorously enforce the legislation related to the energy performance of buildings [1]." The Netherlands as part of the European Union will take part in the efforts to increase energy efficiency of buildings. Historically buildings in the Netherlands are heated by fossil resources extracted from the Dutch subsurface. Most building have central heating systems relying on natural gas.

These factors result in the fact that the Netherlands is accelerating its efforts to transition the heating demand of buildings towards renewable energy. The main challenge lies in the transition of the roughly 6-7 million existing buildings with low energy efficiency that are still relying on natural gas for space heating. For existing buildings the transition is more difficult compared to new built homes since systems that are already in place need to be altered to sustain the same level of comfort at a cost competitive price. Another challenge in the transition are the periods in which little energy can be generated with renewable resources due to lack of wind and/or sunlight.

In cooperation with the Dutch government a feasibility project is started to evaluate the opportunity for heating of existing buildings with renewable energy. This project carries the name 'Energiek Nagele'. The houses were built in the 1950's and currently rely on natural gas for their space heating. The main goal of renewable central heating systems is the reduction of greenhouse gas (GHG) emissions. The advancements in renewable energy technologies and cost reductions enable the start of the transition to renewables based central heating for the built environment in the Netherlands. Though, due to the intermittent nature of renewable energy sources, an energy storage solution is needed to ensure energy availability at all times.

The company Hocosto has proposed a method to overcome such periods by introducing a seasonal sensible heat storage tank installed underground. This storage is able to store heat during periods where energy can be generated for instance during summer and use this heat later to serve the heating demand through a small scale district heating network. This paper aims to investigate whether a neighbourhood can rely on a small scale district heating network with local seasonal heat storage and to compare two different thermal energy harnessing methods to charge the storage tank and find the most cost effective solution. The first system, system 1, relies on solar collectors for its heat generation. The second, system 2, uses an air-water heat pump to move energy/heat from ambient air to the storage tank. Both systems have an USTES to overcome periods where due to lack of wind or sunshine no renewable energy can be collected. The solar collectors experience this effect during cold periods with little sunshine, the heat pump is effected during times with low ambient temperatures.

This paper summarizes the work developed by ter Meulen [2] in the frame of the 'Energiek Nagele' project.

1.1 Thermal energy storage in combination with solar thermal collectors

System 1, presented in Fig. 1, starts by collecting heat in solar thermal collectors during summer. The collector arrays are installed on the rooftop of buildings and connected with the USTES by an insulated district heating network (DHN). Here the energy will be stored as sensible heat in water for later use during winter. A water-water heat pump will be installed using the USTES as its source medium to increase the exergy of the water.

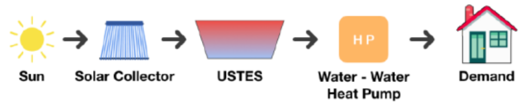

Fig. 1 - System 1, with a solar collector array as main heat source. An USTES is used as heat storage and a water-water heat pump is installed in order to increase the exergy of the water.

1.2 Thermal energy storage using a central heat pump

The alternative system presented in Fig. 2 relies on a central air-water heat pump extracting heat from ambient air and delivering this heat to a heat sink, in this case the USTES. The heat pump will only operate during periods where its coefficient of performance is above a certain threshold. This means the heat pump is turned off during periods of low ambient temperature. During these periods the USTES will cover the heating demand of the households. In this system also a water-water heat pump will be installed to increase the exergy of the water. Photo-voltaic (PV) panels will deliver electricity for the heat pump when possible. However it will not be a fully autonomous system since exchange with the grid will be allowed resulting in a "zero on the meter" system.

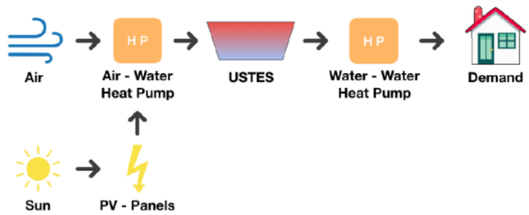

Fig. 2 – System 2, with an air-water heat pump as main heat source. An USTES is used as heat storage and a water-water heat pump is installed in order to increase the exergy of the water.

2. Heating demand of participating households

2.1 Demand profile

The natural gas demand for the 24 participating households in the project 'Karwijhof, Nagele' for the year 2018 is known and displayed in Fig. 3. The graph visualises the natural gas demand of the neighbourhood for one year. However, the natural gas demand profile is not consistent year over year. For instance, demand depends on the demography of the neighbourhood which changes slowly over the years. More significantly does the energy demand depend on the ambient temperatures in winter which may vary greatly over the years. This effect will be discussed in section 2.2.

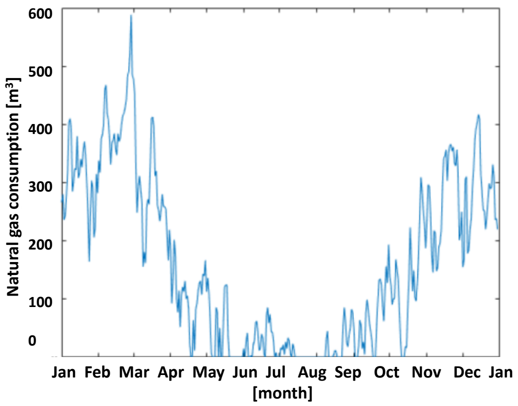

Fig. 3 – Daily gas consumption of the participating 24 users at 'Energiek Nagele' coupled to the outdoor daily mean air temperature measured by the KNMI at Marknesse weather station along the year 2018. The measured total annual gas consumption is 58448 m^3.

The energy demand of the users considered during this study is without any additional measures to improve the energy efficiency of the household. It is not yet known what additional measures can be taken due to the monumental status of the buildings. The monthly energy demand of households in the Netherlands also varies within one year due to seasonal changes. In winter more energy is required for space heating. This results in a higher energy consumption during the cold winter months compared to the warmer summer months. From Fig. 3 a demand profile can be obtained. The figure shows that natural gas consumption peaks in the months November - March and follows a sinusoidal profile. Notice that one of the buildings is a former school which consumes almost 20% of the total.

2.2 Climate effect on energy demand

Climate has a large effect on energy demand for space heating. Therefore, the Dutch meteorological institute (KNMI) uses a definition called "degree days" to account for this climate effect on energy demand. This method is also widely used in literature, for instance by Niessink [3] and Sorknæs [4] among others. Niessink [2] describes a degree day as a day in the year where the outside air temperature is below 18 °C, since only below this temperature a building is assumed to require space heating, otherwise known as the heating limit. Every degree Celsius below this 18 degrees is counted as one degree day. To give an example: if for a given day the outside temperature averaged over 24 hours is 8 degrees, then this accounts for 18-8=10 degree days [3]. The number of degree days gives an indication of the severity of the winter and therefore the need for space heating and its related energy demand. The number of degree days varies greatly over the years. For instance, the (unweighted) difference between 2013 (3078) and 2014 (2385) is 693 degree days where the KNMI climate expectation was 2779 - 2769 degree days respectively. This is a deviation of +11% and -14% respectively from the KNMI expected number of degree days for those years [5]. The degree days are weighted to account for the seasonal changes in solar insolation which contributes to the space heating of a house. Degree-days from November-February are weighted with a factor of 1.1, degree days in March and October have a weight factor of 1 and April-September get a weight factor of 0.8 [6].

2.3 District heating network

The households will be connected to the district heating network (DHN). This DHN will be used to transport the hot water from the heat storage to the houses for space heating and tap water. For this study a traditional two-line network is considered with a supply and return line. The water in the supply line needs to be at a minimum temperature in order to transport enough energy to meet the heating demand, to ensure a certain comfort level, and to ensure the Legionella legislation is met. This translates in the need for a minimum supply or service level temperature of the DHN. The supply temperature is dependent on the energy demand of the households. In general a minimum supply temperature of 70 °C is pre-defined. However, during Autumn and Spring a lower supply temperature is sufficient. Usually the heating temperature is variable from the heating threshold of 18 °C. Though, due to Dutch legionella bacteria legislation it is required for the households to be supplied with water of at least 55 °C for hot tap water production. This results in a relatively flat variable service level with a base temperature of 63 °C. The return flow temperature is constant since with increasing demand the DHN flow rate will increase such that the return temperature remains constant at 40 °C.

The same DHN applies for the two compared systems. The DHN needs to be determined with reasonable accuracy since it impacts on the LCOH. The thermal losses in the pipe network and the electricity consumption of pumps are important parameters since they have impact on the LCOH and the SCOP of the system. The layout of the network is given in Fig. 4.

3. Key performance indicators (KPIs)

The performance of the systems is evaluated based on the levelised cost of heat and on the seasonal coefficient of performance of the system.

3.1 Levelised cost of heat

The levelised cost of heat (LCOH) is defined as the initial investment or capital costs (CAPEX) of the system plus the operational costs (OPEX) divided by the total amount of heat delivered to the households.

Fig. 4 – Layout of the 2-line district heating network (DHN). Participating buildings are indicated in blue, the USTES is indicated in red, and the DHN is indicated by the black lines. Total length of the DHN is 700 m.

$$LCOH = \frac{CAPEX + \sum_{t=1}^{T} \frac{OPEX_t}{(1+r)^t}}{\sum_{t=1}^{T} \frac{E_t}{(1+r)^t}} \quad (1)$$

where T is the total life expectancy of the system (30 year), t is the time in years, r is the discount rate, $OPEX_t$ are the total operating costs in year t , and E_t is the total heat delivered in year t. The discount rate is assumed at 2% since sustainable energy projects generally are subject to low interest rates.

3.2 Seasonal system of performance

The system performance is also based on the seasonal coefficient of performance (SCOP). This represents the ratio between the heat that is delivered to the households and the total electric energy consumed by the system.

$$SCOP = \frac{\sum E_{delivered}}{\sum E_{electricity\ consumed}} \quad (2)$$

4. System design

4.1 System layout and control

For system 1 district heating network heat is generated by solar collectors, stored by a single USTES and has the possibility to use a water - water heat pump when the USTES temperature is below supply temperature level. A schematic overview of the system is given in Fig. 5 (LHS). System 2 consists of a central air - water heat pump for thermal energy generation, the USTES for thermal storage, a water - water heat pump to maximise exergy of the water, and the DHN to supply demand. A schematic overview of the system is given in Fig. 5 (RHS).

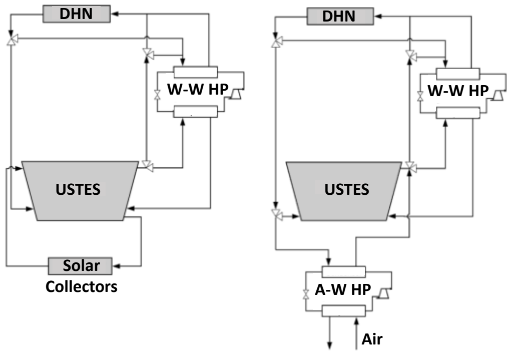

Fig. 5 – LHS: Technical overview of the components making up system 1. Arrows represent piping. The blank triangles represent control valves. RHS: Technical overview of the components in the air-water heat pump based system (system 2).

The system using an air-water heat pump has a control strategy based on the ambient air temperature. If the air temperature ≥ 18 °C then the heat pump will be operational while there is only some tap water demand by the households. The demand will be supplied by the USTES while simultaneously the heat pump is charging the USTES with hot water. If the air temperature is between 10 and 18 °C then there is a space heating demand and the heat pump is operational. The heat pump is charging the USTES. Simultaneously the USTES is discharging into the DHN to meet demand. If the air temperature is lower than the minimal operating temperature of the heat pump then the heat pump is not operational. Heat is supplied directly from the USTES. When the USTES is below supply service level (63 °C) the water - water heat pump will "upgrade" the return heat with energy sourced from the USTES.

The system can discharge into the DHN in three different modes depending on the temperature of the USTES. Due to space limitations these modes will not be discussed here.

4.2 Component modelling

Heat demand The demand is modelled from two input parameters. These are the hourly ambient air temperature provided by the KNMI, and the natural gas consumption of the households provided by the Energiek Nagele project. The two data sets are correlated to obtain the energy demand of the households per degree day, and subsequently degree hour.

USTES Research has shown that in liquid-based, sensible heat storage systems high degrees of stratification can be achieved. This stratification is mostly described using simplified one dimensional models. Cruickshank and Baldwin [7] propose a model of a stratified thermal storage by dividing the tank into N constant volume sections or "nodes". Fig. 6 visualises the node approach applied to the USTES which is a pit storage as proposed by Hocosto. The nodes are assumed to be fully mixed and at uniform temperature. The resolution of the temperature stratification depends on the number of nodes used. The more nodes the higher the resolution will be, but also the longer the computation time. Cruickshank and Baldwin found that 10 nodes result in an accurate resolution with acceptable computation times, this is therefore the number of nodes used during this study. For each node an energy balance is introduced accounting for the thermal losses to its surroundings and for instance, conduction between the nodes. Each node will represent a sensor installed inside the USTES spaced uniformly in the vertical direction at a distance $\Delta z = z/N_{nodes}$ with z de height of the USTES.

To model the USTES the energy balance for each node needs to be considered. Mass flows leave and enter the nodes at different temperatures changing this energy balance. Also, the USTES is heated up by the solar collector array. The result is an energy balance with various components, these are: heat losses, heat conduction, mixing between nodes (convection), solar energy charging, and heat exchange with the DHN. The previous components are visualised in Fig. 6.

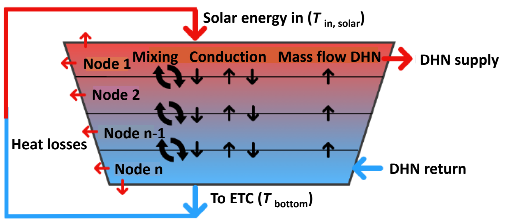

Fig. 6 – Energy flows in the USTES consisting of the heat losses to its surroundings, mixing between nodes, conduction between nodes, mass and heat transport due to solar charging, and mass and heat transport due to heat supply to the users through the DHN.

Solar thermal collectors The quasi dynamic approach proposed by Fischer et al. [8] has been adopted to determine the solar collector thermal output as a function of the local instantaneous radiation data. These data was obtained from the Dutch Meteorological Institute (KNMI). The solar thermal collectors are installed in arrays on the rooftops of the buildings. The rooftops consist of 2 flat surfaces on buildings near the USTES. In this study a separate DHN pipe is assumed to collect heat from the solar collectors and to transport it to the USTES. The solar collectors are installed at a fixed angle of 15 ° oriented 180 ° towards the south. The low inclination angle is imposed since the buildings have a monumental status and the collectors cannot be visible from the street.

Heat pumps The heat pumps have been modelled as proposed in Kiss & Infante Ferreira [9] while the thermodynamic properties of the working fluid (R600a) have been imported into the model from REFPROP (Lemmon et al. [10]). The heat pump has been designed to take full advantage of the large temperature glide of the water flow and includes an internal heat exchanger.

PV panels The performance of the PV panels was obtained as proposed by Smets et al. [11]. The specifications of the Trina Solar Duomax 144 PV panel have been adopted [12].

4.2 Component costs

Table 1 provides a summary of the costs.

Tab. 1 - Cost overview of the system components. In the last column it is indicated whether the costs contribute to the initial capital expenses (CAPEX) or operating costs (OPEX)..

Component	Cost [€]	Capacity	CAPEX/ OPEX
USTES	150	m^3	CAPEX
w-wHeat Pump	500	kW	CAPEX
a-w Heat Pump	450	kW	CAPEX
Evacuated tube collectors	450	m^2	CAPEX
Photovoltaic panels	180	m^2	CAPEX
DHN	150	m	CAPEX
Electricity 0-10000 kWh	0.178	kWh	OPEX
Electricity 10000-2500000 kWh	0.150	kWh	OPEX
Maintenance	1.2%	CAPEX	OPEX

5. Results

The solar collector based system (system 1) has two variable components. These are the USTES volume and the amount of solar collector surface area. The sizing of the air-water heat pump (system 2) is performed by iteration of two variables, the air-water heat pump heating capacity and the USTES volume.

5.1 Optimum LCOH

The optimum LCOH is obtained at its lowest. Fig. 7 (TOP) shows the LCOH of system 1 as function of the USTES volume for different surface areas of the solar collector array. The lowest LCOH is 0.128 €/kWh for an USTES volume of 1600 m^3 and a solar collector area of 800 m^2. The LCOH of the air-water heat pump system (system 2) has a minimum of 0.118 €/kWh at an USTES volume of 1300 m^3 and a heat pump heating capacity of 175 kW. The graph in Fig. 7 (BOTTOM) shows the optimum for the air water heat pump based system.

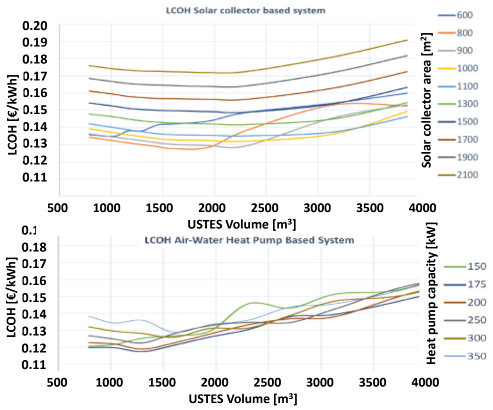

Fig. 7 - LCOH of the system configurations defining an optimum at the lowest point in the graph. Each line of system 1 (TOP) represents a certain solar collector array surface area. The x-axis shows the USTES volume while the y-axis presents the LCOH of the system. For system 2 (BOTTOM) each line represents a certain heat pump heating capacity in kW.

5.2 Optimum Systems COP (SCOP)

The systems seasonal coefficient of performance is optimal when at a maximum value is obtained. This maximum SCOP is theoretically infinite since when no electricity is consumed by the system, no external energy is imported and the system operates fully autonomous. The lower the SCOP the worse the efficiency of the system is. The SCOP of the different system sizes are presented in Fig. 8 with system 1 on top and system 2 at bottom.

For system 1 (Fig. 8, TOP) the SCOP increases with USTES volume and solar collector surface area since auxiliary heating and water-water heat pump operating hours decrease with increasing USTES volume and solar collector surface area.

For system 2 (Fig. 8 BOTTOM) the SCOP optimum approaches a maximum with increasing USTES volume and increasing heat pump capacity. However, the SCOP has a limit related to the COP of the air-water heat pump. The maximum COP of the air-water heat pump based system is 3.1, this is the highest efficiency the system is able to achieve and subsequently the limit to the SCOP of the system.

5.3 CAPEX of systems 1 & 2

The CAPEX of the systems are based on the optimal system configuration as defined in section 5.1. The CAPEX of the solar collector based system (system 1) is 993. k€. The pie chart in Fig. 9 breaks down the cost of components with left system 1 and right system 2. The costs for the DHN are fixed for every configuration and makes up 10% of the total CAPEX of system 1. capacity. Total costs are 493.5 k€.

The CAPEX of the air-water heat pump based system (system 2) is 493.5 k€. From Fig. 9 (RHS) becomes clear that the USTES contributes the largest part of the total CAPEX. The costs for the DHN make up 21% of the total CAPEX of system 2.

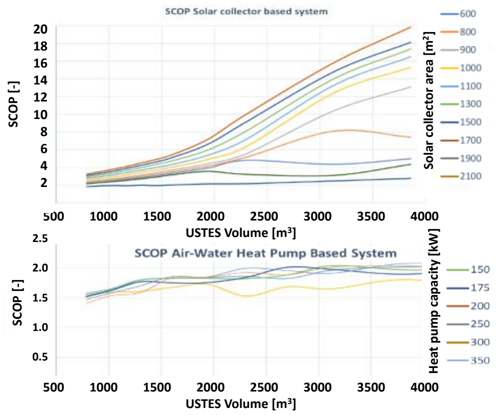

Fig. 8 – TOP: SCOP of the solar collector system configurations increasing with increasing size. Each line represents a certain solar collector array surface area. BOTTOM: Each line represents an installed heat pump heating capacity in kW.

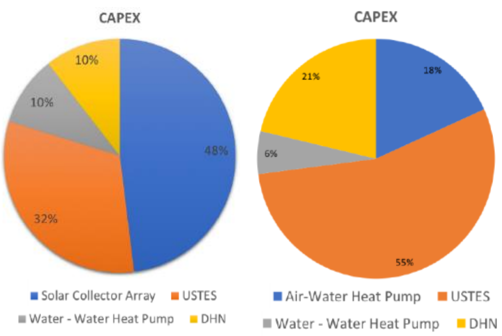

Fig. 9 – LHS: CAPEX cost share of the components for solar collector based system (system 1) with 2100 m³ USTES and 1060 m² solar collectors. Total costs are 993. K€. RHS: CAPEX cost share of the components for the heat pump based system (system 2) with 1800 m³ USTES and 200 kW air-water heat pump heating

5.4 Optimum LCOH of autonomous systems

Both systems 1 & 2 depend on electricity sourced from the grid. To increase the autonomy and renewable share of the system, PV panels can be installed. The solar collector based system does not have the entire rooftop area left since the solar collectors are already taking up a large part of the available space. The heat pump based system does have the entire rooftop area available for additional PV panels. One concern is the mismatch in time between consumption and generation. These systems are therefore not aimed to be fully autonomous but "zero on the meter", meaning the electricity generation is offset to the consumption using the general electricity grid as a "storage".

By installing a PV array the entire electricity use of the systems is compensated. Part of the effective rooftop area, totalling 1344 m², will be used for the placement of the PV array. This results in an increase of the SCOP to infinity since all energy consumed by the system is also generated within the system. The cost of the PV panels increases the CAPEX of the systems and subsequently the LCOH reaches a new optimum.

For the solar collector based system (system 1) including PV the optimal LCOH is 0.126 €/kWh with a solar collector surface area of 1000 m², a PV surface area of 333 m² and a USTES volume of 3141 m³. Fig. 10 (top) presents the LCOH for different component configurations. The LCOH of this system is limited by the rooftop area available.

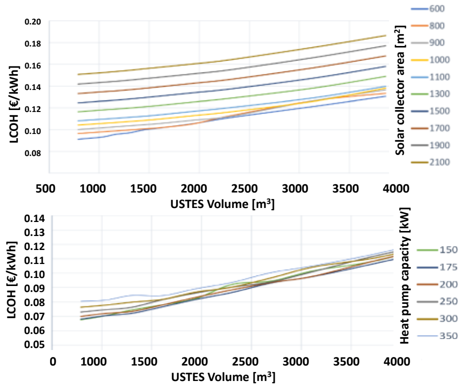

Fig. 10 – Autonomous systems with PV array installed on roofs. TOP: LCOH of the solar collector based system (system 1) including a PV array. BOTTOM: LCOH of the air-water heat pump system (system 2) including a PV array.

The air-water heat pump system consumes more energy compared to the solar collector based system and therefore needs more surface area of PV panels to reach "zero on the meter" autonomy. Fig. 10 (BOTTOM) presents the LCOH for the air-water heat pump system while all electricity use is offset by PV panels. The optimal LCOH for this system is 0.094 €/kWh at a USTES volume of 2709 m³ and a heat pump heating capacity of 250 kW. To ensure all electricity is produced on site a PV array of 1343 m² is needed. This is considered the optimal configuration since the only relevant KPI is the LCOH. The autonomy of the system is equal for all configurations since all electricity is produced by the system. The system is constraint by the rooftop area available. With additional PV panels the LCOH can be reduced further.

5.5 CAPEX of autonomous systems 1 & 2

The CAPEX share for each component of the system is presented in Fig. 11 with system 1 on the LHS and system 2 on the RHS. The PV array entails 5% of the total CAPEX of system 1. The CAPEX of system 1 totals 1182. k€. The CAPEX of the system 2 is 882. k€ and is presented in the RHS of Fig. 11. The PV array entails 27% of the total CAPEX of system 2.

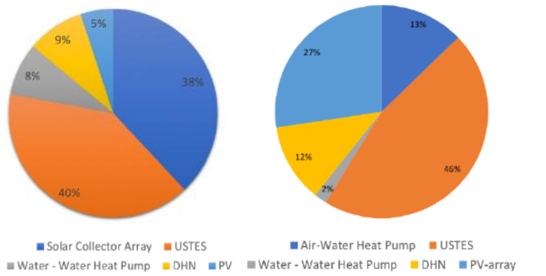

Fig. 11 – LHS: Pie chart of the CAPEX of the solar collector based system including PV. The system consists of 1000 m² of solar collectors, 333 m² of PV panels and 3141 m³ of USTES. RHS: Pie chart of the CAPEX of the air-water heat pump system including PV. The system consists of an USTES of 2709 m³, a 250 kW air-water heat pump, and a 1343 m² PV array.

5.6 Optimal system configuration

The optimal system configuration and sizing for the solar collector based system with PV array is based on "Zero on the meter" at the lowest possible cost while taking into account the rooftop area constraint. This results in a system with 1000 m² of solar collector area, 3141 m³ of USTES volume, and 333 m² of PV panels. The LCOH of the system is 0.126 €/kWh. The LCOH can come down further by installing additional PV panels. However, the rooftop surface area constraints the PV array size. The optimal system configuration and sizing for the heat pump based system with PV array is also determined to achieve "zero on the meter" at lowest cost. This results in a system with 250 kW of air-water heat pump heating capacity, 2709 m³ of USTES volume, and 1343 m² of PV panels. This results in a LCOH of 0.094 €/kWh. Again the LCOH can come down further if not for the rooftop area constraint.

The temperature of the nodes in the USTES over the years is presented in Fig. 12 (TOP) for system 1. From the graph can be seen that the temperature fluctuations are not the same every year but do follow a similar trend. From the figure follows that not all energy comes from the solar collectors but some auxiliary heating is needed with this system sizing. These are the periods for which the USTES reaches a temperature of 5 °C. This implies that using additional solar collectors and USTES volume to ensure demand are more expensive compared to the use of auxiliary heating. This is due to the relatively low cost of electricity and it results in a larger investment, operating and maintenance costs. By installing an PV array the auxiliary heating can also be considered renewable.

The temperature profile of the USTES over the same period is presented in Fig. 12 (BOTTOM) for system 2. To be certain the heat pump is only operating when energy can be added to the USTES, it only operates when the temperature of the bottom node of the USTES is below 80 °C and when there is a return mass flow from the DHN at 40 °C. This translates in the fact that the bottom node appears to be fluctuating between 80-90 °C. From Fig. 12 (BOTTOM) also follows that in the years 2017 and 2018 some auxiliary heating is needed. This auxiliary heating can be prevented by installing more m³ of USTES. However, based on the KPI's apparently it is favourable to have some auxiliary heating since it leads to a lower LCOH compared to installing additional USTES volume.

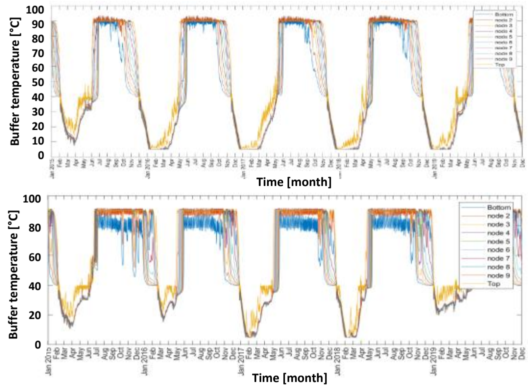

Fig. 12 – TOP: Temperature of the nodes in the USTES during a five year time period with 2100 m³ USTES and 1060 m² solar collectors. BOTTOM: Temperature profile of the nodes in the USTES during the same period with 1800 m³ USTES and 200 kW air-water heat pump heating capacity.

6. Discussion

6.1 Economic feasibility of proposed systems

The results show that it is feasible, both technically and economically, to have a small scale district heating network operating year round based on renewable energy combined with a local seasonal heat storage. To ensure the system is fully renewable a PV array is needed.

6.2 Cost competitiveness

Traditional heat generated by burning natural gas using a HR-boiler operating at a seasonal efficiency of 90% costs 0.088 €/kWh excluding capital costs (the initial costs of the HR-boiler) since the system is already in place. This is the business as usual in the Netherlands for the majority of households. Therefore, this price of heat is the benchmark for renewable heating systems.

The systems including a PV array produce an LCOH of 0.126 €/kWh for the solar collector based system including PV and 0.094 €/kWh for the air-water heat pump based system including PV. The latter is the most competitive with the business as usual case of all system configurations but still cannot compete. With more rooftop area available the systems with PV are able to be cost competitive with the base case.

7. Conclusions

A model to predict the performance of DHN based on renewable resources which make use of high temperature sensible pit heat storage tanks has been developed and implemented in MATLAB/Simulink. The model has been used to optimize the size of the renewable resources and pit storage to reach as low as possible LCOH for a group of 24 buildings in Nagele.

Under the assumptions made, the following has been concluded: The best performance is obtained for the system with an air source based heat pump which delivers heat to the hot pit storage when the environmental temperature is sufficiently high. The air-water heat pump has a heating capacity of 250 kW, the USTES a volume of 2709 m³ and the PV panels an area of 1343 m². The LCOH of the system is 0.094 €/kWh which is only slightly higher than the LCOH with conventional HR-boilers in 2020 (0.088 €/kWh).

Data access statement

The datasets generated during and/or analysed during the current study are not publicly available because MSc thesis [2] is under embargo but will be available at the end of embargo period.

8. References

[1] European Commission. (2019) The European Green Deal. page 9. retrieved from https://ec.europa.eu/info/sites/info/files/european-green-deal-communication_en.pdf

[2] ter Meulen B.P. Underground heat storage. M. Sc. Thesis. Delft University of Technology. 2020; 127 p.

[3] Niessink, R.J.M. (2017) Temperature correction – A Sensitivity Analysis. ECN Amsterdam 2017. https://publicaties.ecn.nl/PdfFetch.aspx?nr=ECN-N--17-039 .

[4] Sorknæs, P. Simulation method for a pit seasonal thermal energy storage system with a heat pump in a district heating system. Energy. 2018;152:533-538.

[5] Centraal Bureau van de Statistiek. Energieverbruik van particuliere huishoudens. 2018. retrieved from https://www.cbs.nl/nl-nl/achtergrond/2018/14/energieverbruik-van-particulierehuishoudens

[6] Centraal Bureau van de Statistiek. Energie - Cijfers. 2018. retrieved from https://longreads.cbs.nl/trends18/economie/cijfers/energie/#huishoudelijk-energieverbruik

[7] Cruickshank, A.C., Baldwin, C. Sensible Thermal Energy Storage: Diurnal and Seasonal. Storing Energy. 2016;1:91-311.

[8] Fischer, S., Muller-Steinhagen, H., Perers, B., Bergquist, P. (2017) Collector test method under quasi-dynamic conditions according to European Standard EN 12975-2. retrieved from http://www.estif.org/solarkeymark/Links/Internal_links/wp1a/m3wp1ad3.pdf .

[9] Kiss, A.A., Infante Ferreira, C.A. (2017) Heat Pumps in Chemical Process Industry. CRC Press 2017. isbn 978-1-4987-1895-0.

[10] Lemmon, E.W., Bell, I.H., Huber, M.L., McLinden, M.O. (2018) NIST Standard Reference Database 23: Reference Fluid Thermodynamic and Transport Properties-REFPROP, Version 10.0, National Institute of Standards and Technology. 2018. doi: http://dx.doi.org/10.18434/T4JS3C. https://www.nist.gov/srd/refprop

[11] Smets, A., Jager, K., Isabella, O., Swaaij van, R., Zeman, M. (2016) Solar Energy 2016. UIT Cambridge Ltd. isbn: 9781906860325

[12] Trina Solar. Datasheet: Trina Solar DUOMAX dual glass 144 half-cell module. 2019. Retrieved from https://static.trinasolar.com/sites/default/files/PS-M%20A%20Datasheet_Duomax_DEG15H.20%28II%29_NA_2019_A_0.pdf